Communications on Applied Nonlinear Analysis
ISSN: 1074-133X
Vol 32 No. 10s (2025)

The Investigation of the Shear Capacity of Fiber Reinforced Polymer (FRP) Deep Beams.

Anand Kamble[1], Ashutosh Pandey[2]

[1.] Post Graduate Student, Department of Civil Engineering

[2.] Ashutosh Pandey, Assistant Professor, Department of Civil Engineering Kalinga University Raipur, Chhattisgarh, India.

Article History:

Received: 12-01-2025

Revised: 15-02-2025

Accepted: 01-03-2025

Abstract:

The use of fiber-reinforced polymer (FRP) reinforcement in deep beams is expected to grow due to its ability to address corrosion issues in concrete structures.

FRP bars offer advantages such as high strength-to-weight ratio, fatigue resistance, and non-corrosive properties. These bars are emerging as a viable alternative to traditional steel reinforcement. Certain structures like underground tunnels, transfer girders, and bridges often require large concrete sections with low shear span-to-depth ratios (a/d), which generally transfer load through arch action. However, there is no simple method to estimate the shear strength of such members, and current strut-and-tie models are complex and yield varying results.

A simplified approach to estimate shear capacity is needed for engineers. The shear span-to-depth ratio (a/d) significantly impacts the shear strength of FRP-reinforced members. Based on research, modifications to design codes, particularly for deep beams (a/d <2.5) and FRP-reinforced concrete members, have been proposed by the American Concrete Institute (ACI) and Canadian Standards Association (CSA).

This paper investigates the shear capacities of two deep beams, one simply supported and reinforced with carbon fiber-reinforced polymer (CFRP) and the other continuous and reinforced with glass fiber-reinforced polymer (GFRP) bars.

Both were analyzed using ABAQUS/CAE 2017 software, and a sensitivity study was conducted comparing results with experimental data from existing studies.

The shear span-to-depth ratio varied from 1.0 to 2.5. The results indicated that increasing the ratio significantly reduced load capacity, and continuous beams showed higher load capacity than simply supported beams.

Keywords: Fiber-Reinforced Polymer (FRP), Deep Beams, Shear Capacity, Corrosion Resistance, FRP Reinforcement, Concrete Structures, Strut-and-Tie Models, Shear Span-to-Depth Ratio (a/d), Carbon Fiber-Reinforced Polymer (CFRP), Glass Fiber-Reinforced Polymer (GFRP).

1.0 Introduction

General

The behavior of Fiber-Reinforced Polymer (FRP) deep beams is complex and influenced by numerous factors, including:

- Clear span-to-depth ratio (ln/d)

- Shear span-to-depth ratio (a/d)

- Loading type and position
- Tensile steel percentage and web reinforcement
- Support zone width and main reinforcement anchorage
- Concrete strength and additional materials like fibers

1.1 Deep Beams

Deep beams are structural elements with spans comparable to their depths. According to Indian code IS 456: 2000, a beam is considered a deep beam if:

- The effective span-to-depth ratio (Leff/D) is less than 2.0 for simply supported deep beams.
- The effective span-to-depth ratio (Leff/D) is less than 2.5 for continuous deep beams.

1.2 Fiber Reinforced Polymers (FRP)

FRP is a composite material consisting of high-performance fibers embedded in a polymer matrix. This combination of materials with different forms and compositions on a macro scale creates a unique material with enhanced properties.

Components of FRP

- Fibers: Carbon, glass, and aramid fibers are commonly used in FRP.
- Polymers: Epoxy, vinyl ester, polyester, and phenol formaldehyde resins are typical polymer matrices used in FRP.

In contrast, the American code ACI 318-08 (2008) defines deep beams as those with a clear span-to-depth ratio of 4.0 or less.

1.3 Fiber Performance in Aggressive Environments

The durability of fibers in harsh environments is crucial for their applications. Here's a brief overview of each fiber type's performance:

- Carbon and Aramid Fibers: Excellent chemical resistance.
- Glass Fibers: Susceptible to damage in alkaline environments.
- UV Resistance:
    - Carbon and Glass Fibers: Unaffected by UV rays.
    - Aramid Fibers: Lose color and strength when exposed to UV rays.

1.4 Applications of Fiber Reinforced Polymers (FRP)

FRPs are versatile materials with diverse applications:

- Ballistic Amour: FRPs are commonly used in protective gear.
- Key Industries:
    1. Aerospace

2. Automotive
3. Construction
4. Consumer Goods
5. Protective Equipment

1.5 Benefits of Fiber Reinforced Plastics (FRP)

FRP offers several advantages, including:

1. Lightweight: FRP is significantly lighter than traditional materials.
2. High Strength: FRP exhibits exceptional strength-to-weight ratio.
3. High Modulus of Elasticity: FRP has a high stiffness, making it ideal for structural applications.
4. Fatigue Resistance: FRP shows excellent resistance to fatigue failure, ensuring durability.
5. Corrosion Resistance: FRP provides good resistance to corrosion, reducing maintenance needs.

1.6 Limitations of Fiber Reinforced Plastics (FRP)

While FRP offers several benefits, it also has some significant drawbacks:

1. Low Transverse Strength: FRP's strength perpendicular to the fibers is significantly lower (up to 5%) than its longitudinal strength.
2. Brittle Failure: FRP can fail suddenly and without warning, unlike metals which often exhibit ductile behavior.
3. High Cost: FRP materials and manufacturing processes can be expensive.
4. Complex Design: Designing components with FRP requires specialized expertise and complex analysis.
5. Specialized Manufacturing and Testing: Producing and testing FRP components demands highly specialized equipment and expertise.

2.0 Literature Review

This literature review provides an overview of existing research on the behavior of FRP-reinforced concrete deep beams, highlighting key findings, methodologies, and areas for future research.

2.1 Material Properties and Beam Configurations .

Ehab El-Salakawy et al.2002

Investigated the behavior of FRP-reinforced concrete beams with varying material properties and beam configurations.

Ahmed K. El-Sayed et al.2002

Explored the effects of reinforcement ratio, modulus of elasticity, and shear span-to-depth ratio on the shear behavior of FRP-reinforced concrete deep beams.

2.2 Strengthening and Repair 2008

Tamer El Maaddawy and Sayed Sherif Demonstrated the effectiveness of externally bonded CFRP sheets in strengthening RC deep beams with openings.

A Zaher

Investigated the use of CFRP and GFRP sheets for shear strengthening of RC deep beams, highlighting significant improvements in ultimate loads.

2.3 Shear Behavior and Design

Ahmed Sabry Farghaly et al.2013

Investigated the shear behavior of FRP-reinforced concrete deep beams, highlighting the importance of longitudinal reinforcement ratio and concrete compressive strength.

Ahmed M. Mohamed et al.2013

Explored the effects of shear span-to-depth ratio on the behavior of GFRP-reinforced concrete deep beams.

2.4 Analytical and Numerical Modeling.

Matthias F. et al.2018

Developed a modeling approach based on the strut-and-tie method for designing FRP-reinforced concrete deep beams.

Mansoor Ahmed Abdullah et al.2018

Presented a numerical analysis using ANSYS to model the behavior of lightweight aggregate reinforced concrete deep beams strengthened with CFRP.

2.5 Future Research Directions

The literature review highlights the need for further research on the behavior of FRP-reinforced concrete deep beams, including:

1. Investigating the effects of varying material properties and beam configurations.

2. Developing more accurate analytical and numerical models.

3. Exploring the use of FRP for strengthening and repair.

4. Investigating the behavior of FRP-reinforced concrete deep beams under different loading conditions.

3.0 Modeling in ABAQUS

Introduction

This chapter presents the modeling procedure for simply supported deep beams and continuous deep beams using ABAQUS CAE/STANDARD software. ABAQUS, a commercial finite element software package, is a powerful tool employed in various fields of investigation.

3.1 Modeling Procedure Overview

Figure 1 Order of processing in ABAQUS

The modeling process in ABAQUS involves four primary stages:

1. Pre-processing: Defining the physical problem, creating the model, and assigning properties.

2. Evaluation and Simulation: Running the analysis and simulating the behavior of the model.

3. Post-processing: Visualizing and interpreting the results of the analysis.

By utilizing ABAQUS, this study aims to investigate the behavior of simply supported deep beams and continuous deep beams, providing valuable insights into their structural performance.

3.2 Pre-Processing, Analysis, and Post-Processing

The finite element analysis in ABAQUS involves three primary stages: pre-processing, analysis, and post-processing.

Pre-Processing

In this stage, the physical problem is defined, and an ABAQUS input file is created. The model is created, and properties, steps, interactions, and other modules are assigned.

Analysis

Any necessary corrections are made, and the data check analysis is performed. Once the analysis completes with no error messages, the analysis itself is run.

Post-Processing

Post-processing is crucial due to the various important data created during a simulation. The Visualization module of Abaqus/CAE enables graphical representation of results using various methods, including:

Deformed shape plots, Contour plots, Vector plots, Animations & X-Y plots.

Tabular reports of output data can also be plotted. Once the job is finished successfully, the results can be visualized using the Visualization module.

3.3 Introduction to ABAQUS

ABAQUS is a suite of powerful engineering simulation programs based on the finite element method. It can solve problems ranging from simple linear analyses to complex nonlinear simulations.

3.4 Key Features of ABAQUS

- Extensive library of elements to model various geometries

- Comprehensive list of material models to simulate behavior of typical engineering materials

- Capable of simulating diverse problems, including heat transfer, mass diffusion, and piezoelectric analysis

- Simple to use, with a wide range of capabilities

- Automatically chooses load increments and convergence tolerances in nonlinear analyses.

3.5 Finite Element Modeling of Deep Beams using ABAQUS/CAE

To model the deep beam using ABAQUS/CAE, the following modules were utilized:

a) Part Module A two-dimensional profile of the deep beam was sketched, and a part representing the deep beam was created.

b) Property Module Material properties and section properties of the beam were defined.

c) Assembly Module

The model was assembled, and sets were created.

d) Step Module

The analysis procedure and output requests were configured.

e) Load Module

Loads and boundary conditions were applied to the beam.

f) Mesh Module

The beam was meshed to prepare it for analysis.

g) Job Module

A job was created, and the model was submitted for analysis.

h) Visualization Module

The visualization module was used to view the model and results of the analysis.

By utilizing these modules, a comprehensive finite element model of the deep beam was developed, enabling the analysis of its structural behavior under various loads and conditions.

4.0 Creating a Part

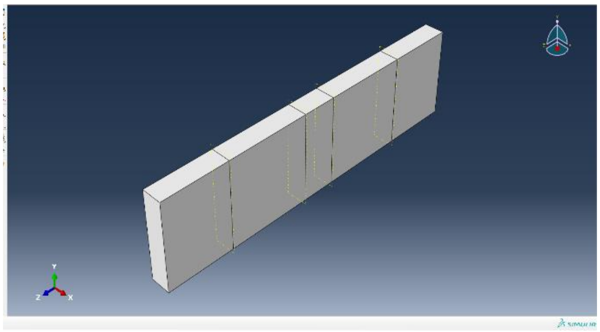

Figure 2 Isometric View of the Simply Supported Deep Beam.

Figure 3 Isometric view of the CFRP Longitudinal Bar

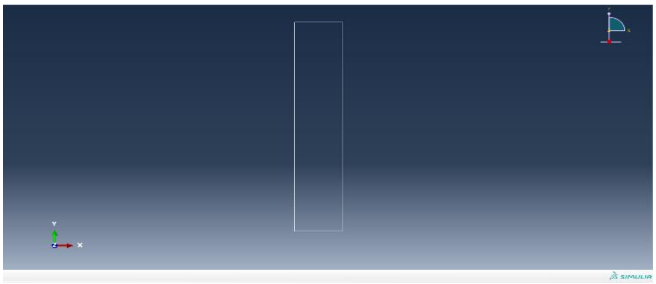

Figure 4 Isometric view of the CFRP stirrup Bar for SSDP

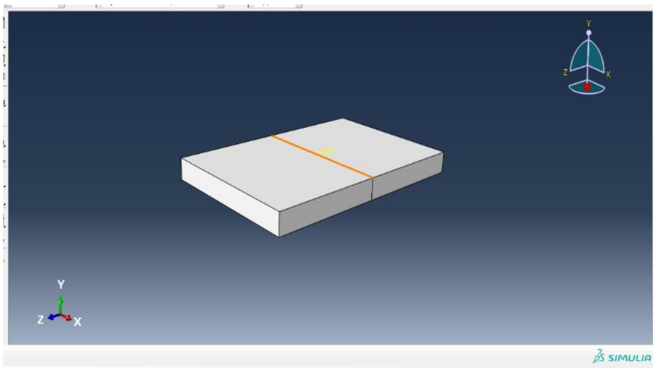

Figure 5 Isometric view of the Steel Support plate of SSDB

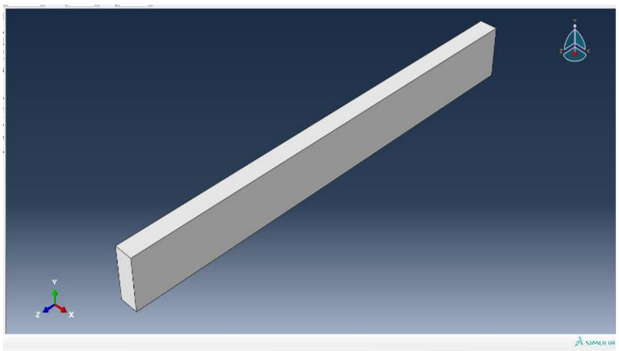

Figure 6 Isometric view of the Continuous Deep Beam.

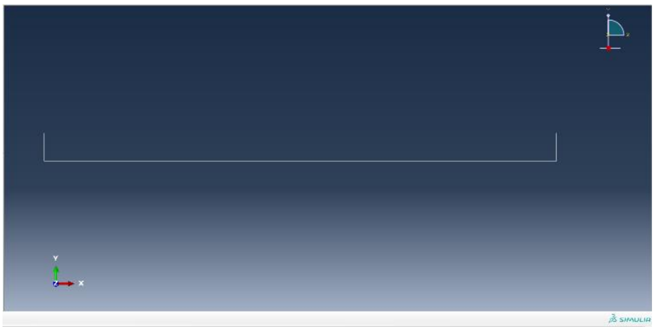

Figure 7 Isometric view of the GFRP longitudinal bar for Continuous deep beam.

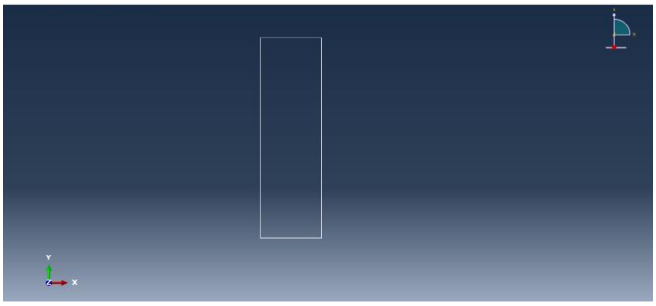

Figure 8 Isometric view of the GFRP stirrup bar Continuous deep beam.

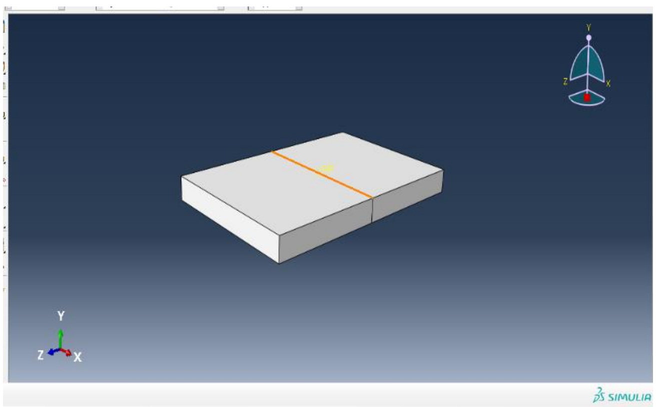

Figure 9 Isometric view of the support of Steel plate for Continuous deep beam.

To model the deep beam components, a three-dimensional, deformable solid body was created for each part, including the deep beam, longitudinal bar, stirrups, and support steel plate.

4.1 Modeling Procedure

1. Sketching: A two-dimensional profile of each part was sketched, using a rectangle as the base shape.

2. Extrusion: The two-dimensional profile was extruded to create a three-dimensional solid body.

3. Abaqus/CAE Sketcher: Abaqus/CAE automatically entered the Sketcher mode when each part was created.

4.2 Deep Beam Components

The following components were modeled:

1. Simply Supported Deep Beam

2. CFRP Longitudinal Bar.

3. CFRP Stirrup Bar.

4. Steel Support Plate.

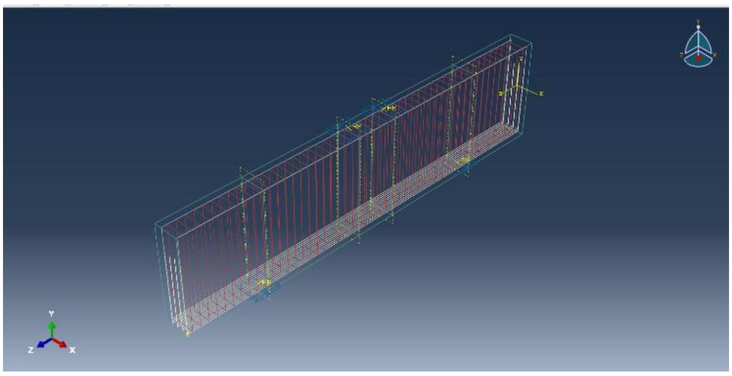

Figure 10 Assembly of CFRP Longitudinal bars and stirrups.

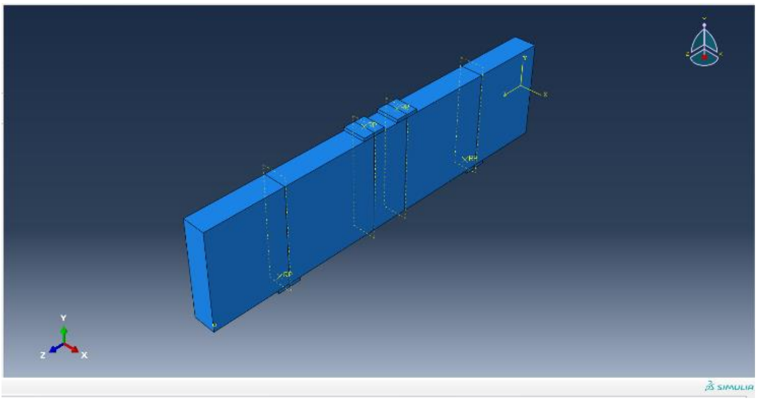

Figure 11 Assembly of Simply supported concrete deep beam, CFRP reinforcement and bearing plates.

4.3 Continuous Deep Beam Components

Similarly, the following components were modeled for the continuous deep beam:

1. Continuous Deep Beam

2. GFRP Longitudinal Bar.

3. GFRP Stirrup Bar.

4. Steel Support Plate.

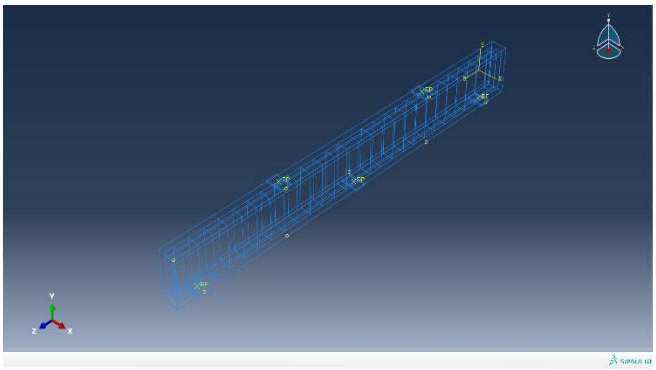

Figure 12 Assembly of GFRP Longitudinal bars and stirrups for continuous deep beam.

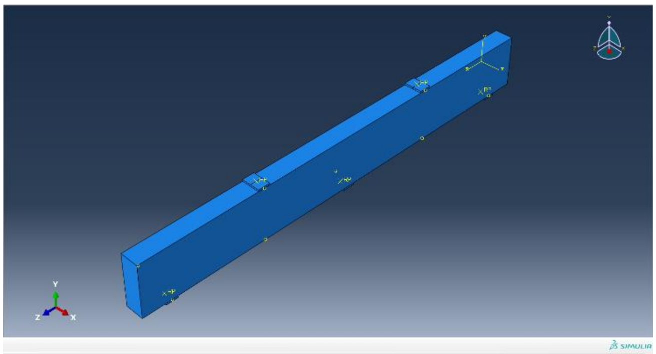

Figure 13 Assembly of continuous concrete deep beam, CFRP reinforcement and bearing plates.

5.0 Creating a Material

To define material properties, a section is assigned in the Property module, which contains information about the properties of a part, including material definition and cross-sectional geometry.

5.1 Material Property Definition

This module is used to define various material properties, such as:

- Elastic modulus (E)

- Poisson's ratios

Communications on Applied Nonlinear Analysis
ISSN: 1074-133X
Vol 32 No. 10s (2025)

- Yield stresses

- Density

- Concrete damage plasticity

- Plastic stress

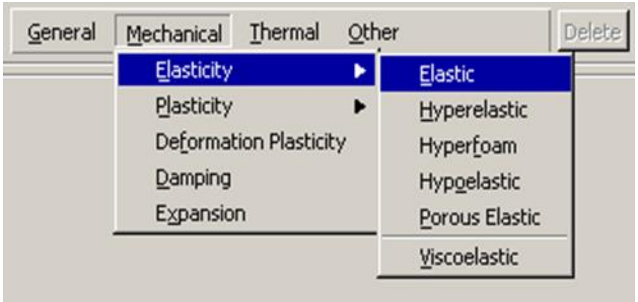

Figure 14 Defining Density of Concrete

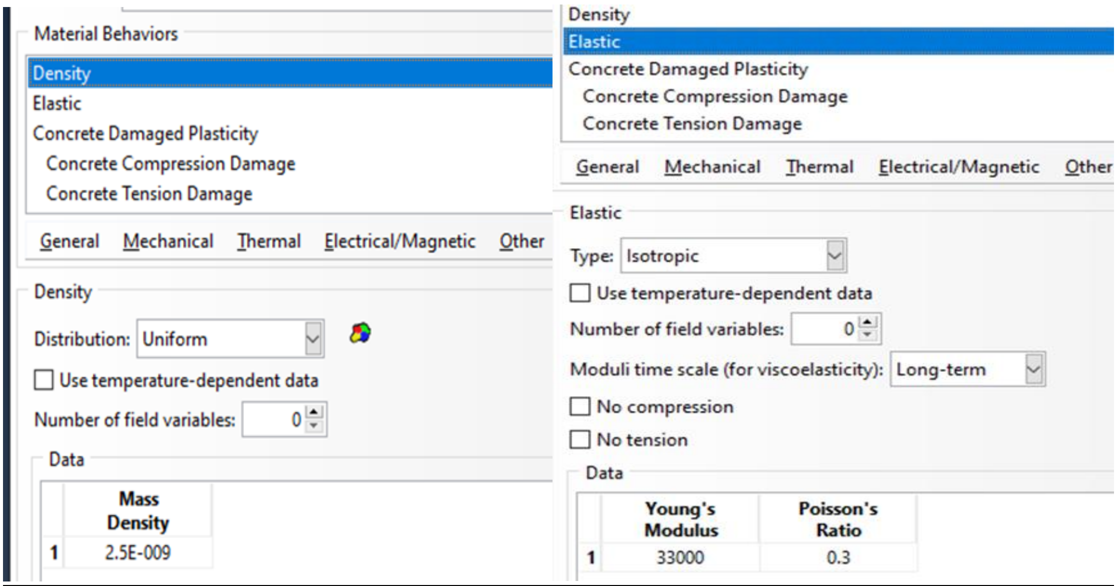

Figure 15 Defining Elasticity of Concrete

Material Models

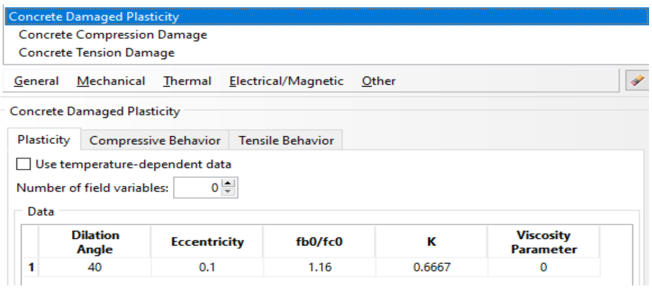

Figure 16 Defining Concrete Damage Plasticity.

Communications on Applied Nonlinear Analysis
ISSN: 1074-133X
Vol 32 No. 10s (2025)

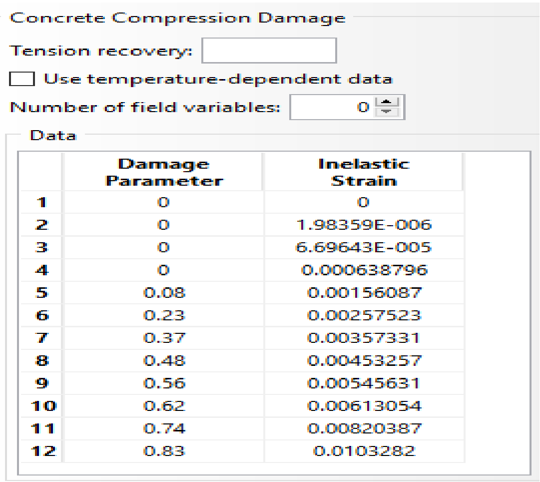

Concrete Compression Damage

Tension recovery:

Use temperature-dependent data

Number of field variables: 0

Data

	Damage Parameter	Inelastic Strain
1	0	0
2	0	1.98359E-006
3	0	6.69643E-005
4	0	0.000638796
5	0.08	0.00156087
6	0.23	0.00257523
7	0.37	0.00357331
8	0.48	0.00453257
9	0.56	0.00545631
10	0.62	0.00613054
11	0.74	0.00820387
12	0.83	0.0103282

Figure 17 Concrete Compression Damage.

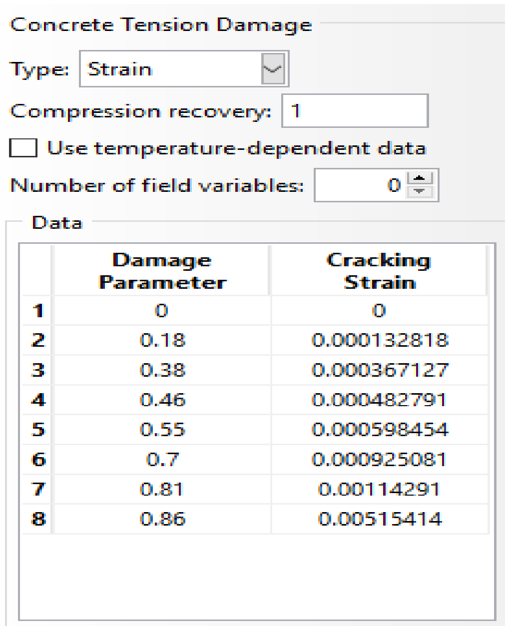

Concrete Tension Damage

Type: Strain

Compression recovery: 1

Use temperature-dependent data

Number of field variables: 0

Data

	Damage Parameter	Cracking Strain
1	0	0
2	0.18	0.000132818
3	0.38	0.000367127
4	0.46	0.000482791
5	0.55	0.000598454
6	0.7	0.000925081
7	0.81	0.00114291
8	0.86	0.00515414

Figure 18 Concrete Tension Damage.

5.2 The following material models were defined:

- Elasticity of concrete
- Concrete damage plasticity (CDP) model
- Concrete compression damage
- Concrete tension damage

5.3 Material Property Values

Data values for elastic and plastic material properties were entered for the following models:

Data

	Yield Stress	Plastic Strain
1	1030.08	0
2	1184	0.0189

Figure 19 Plasticity of 15mm diameter GFRP bar

Data

	Young's Modulus	Poisson's Ratio
1	63700	0.3

Figure 20 Plasticity of 20mm diameter GFRP bar

Data

	Yield Stress	Plastic Strain
1	961.35	0
2	1105	0.0173

Figure 21 Elasticity of 20mm diameter GFRP bar

Data

	Young's Modulus	Poisson's Ratio
1	62600	0.3

Figure 22 Elasticity of 15mm diameter GFRP bar

Data

	Yield Stress	Plastic Strain
1	1652.13	0
2	1899	0.0132

Figure 23 Plasticity of 12.7mm diameter CFRP bar

Data

	Young's Modulus	Poisson's Ratio
1	144000	0.3

Figure 24 Elasticity of 12.7mm diameter CFRP bar

Data

	Mass Density
1	7.85E-009

Figure 25 Density of lower and upper bearing plates.

5.4 Defining Section Properties

Defining and Assigning Section Properties

Section properties can be defined to characterize the behavior of a part. After creating a section, it can be assigned to the part in the current viewport using one of two methods.

5.5 Defining a Homogeneous Solid Section

A homogeneous solid section is the simplest type of section, consisting of a material reference and a plane stress/plane strain thickness.

5.5.1 Steps to Define a Homogeneous Solid Section:

1. Create a Section: Double-click the Sections container in the Model Tree to create a section, opening the Create Section dialog box.

2. Name the Section: Name the section, e.g., "Simply Supported Deep Beam and Continuous Deep Beam".

3. Select Category and Type: Accept Solid as the default category and Homogeneous as the default type.

4. Edit Section Properties: In the Edit Section dialog box:

- Accept the default material selection (Steel).
- Accept the default plane stress/strain thickness value (1).

By following these steps, a homogeneous solid section can be defined and assigned to the part, enabling the analysis of its behavior.

Communications on Applied Nonlinear Analysis
ISSN: 1074-133X
Vol 32 No. 10s (2025)

5.5.2 Assigning Section Properties and Assembling the Model

Assigning Section Properties to Deep Beams

To assign the section properties to the deep beams:

1. Expand Part Branch: In the Model Tree, expand the branch for the part named Beam.

2. Access Section Assignments: Double-click Section Assignments in the list of part attributes.

3. Select Region: Click on the beam to select the region for section assignment.

4. Accept Selected Geometry: Click "Done" to accept the selected geometry.

5. Assign Section: Accept the default selection of Beam Section as the section to be assigned.

5.5.3 Assembling the Model

Each part created in ABAQUS has its own coordinate system and is independent of other parts. To assemble the model:

- Create Instances: Create instances of parts and position them relative to each other in a global coordinate system.

- Independent or Dependent Instances: Instances can be independent or dependent, affecting meshing and analysis.

The Assembly module enables the creation of instances and positioning them in a global coordinate system, forming a single assembly. Part assemblies can also be imported from other software, combining multiple parts into a single part. After creation of part Assembly of FRP longitudinal bar, stirrups and concrete beam should be done as follows

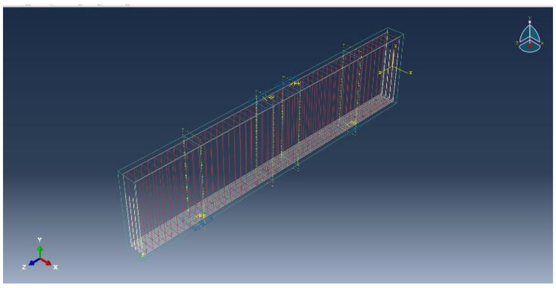

Figure 26 Assembly of CFRP Longitudinal bars and stirrups

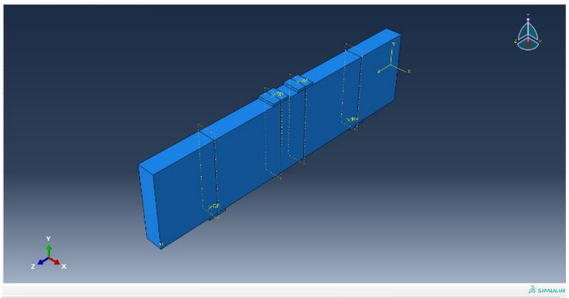

Figure 27 Assembly of Simply supported concrete deep beam, CFRP reinforcement and bearing plates

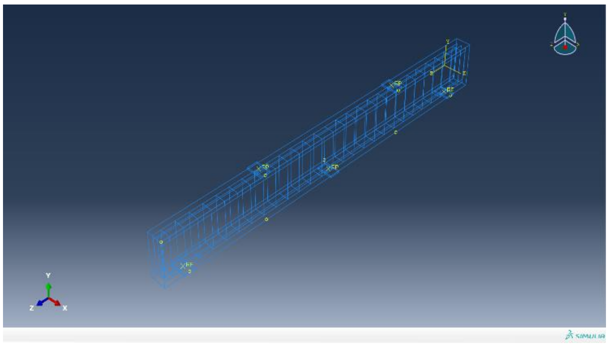

Figure 28 Assembly of GFRP Longitudinal bars and stirrups for continuous deep beam

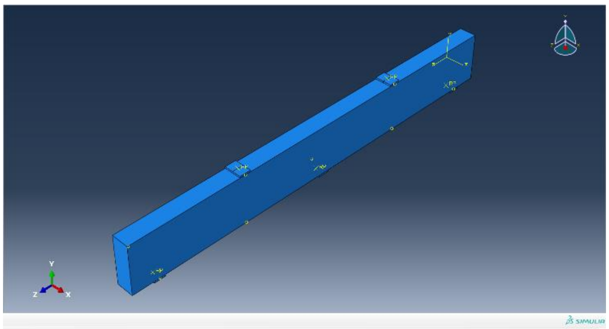

Figure 29 Assembly of continuous concrete deep beam, CFRP reinforcement and bearing plates

5.5.4 Modeling and Analysis of Deep Beams using ABAQUS/CAE

Defining Analysis Steps

With the part created, analysis steps can be defined. For this model, two steps are created:

1. Initial Step: Apply boundary conditions to constrain the bottom lower bearing plate and upper bearing plate of the simply supported deep beam and continuous deep beam.

2. Dynamic Explicit Analysis Step: Apply a pressure load to the top face of the beam.

Interaction Module

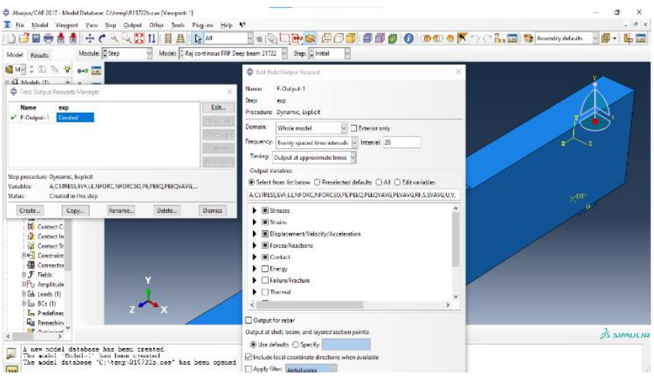

Figure 30 Creating step and Field output request to the beam

In the Interaction module, thermal and mechanical interactions of the model are specified, including:

- Contact between surfaces

- Constraints, such as equations, ties, and rigid bodies

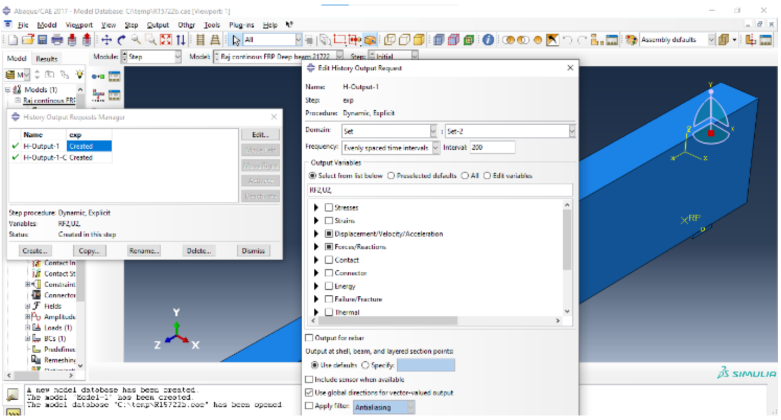

Figure 31 Applying Boundary Conditions and Loads

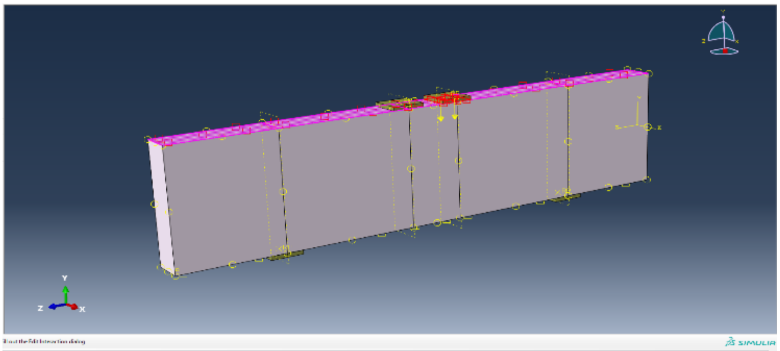

Figure 32 Interaction of Simply Supported Deep Beam

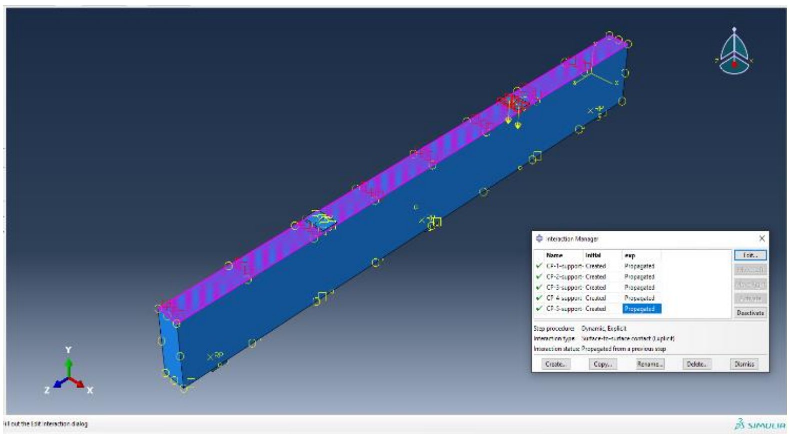

Figure 33 Interaction of Contiguous deep beam

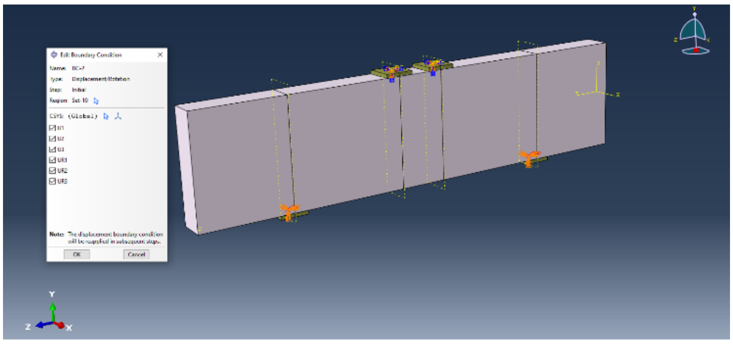

Figure 34 selecting the region on which to apply a boundary condition & Pressure load to simply supported beam

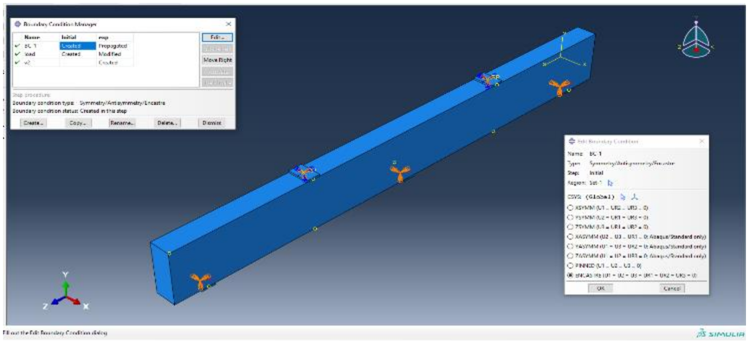

Figure 35 Selecting the Region on Which to Apply a Boundary Condition and Pressure Load to Continuous Deep Beam

The Load module is used to assign boundary conditions, loads, and predefined fields. Boundary conditions and loads are step-dependent objects.

Meshing the Model

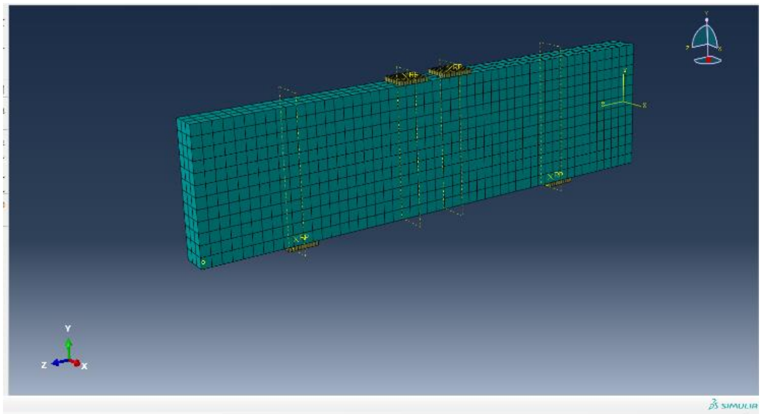

Figure 36 Meshing of simply supported deep beam, FRP reinforcement and bearing plates

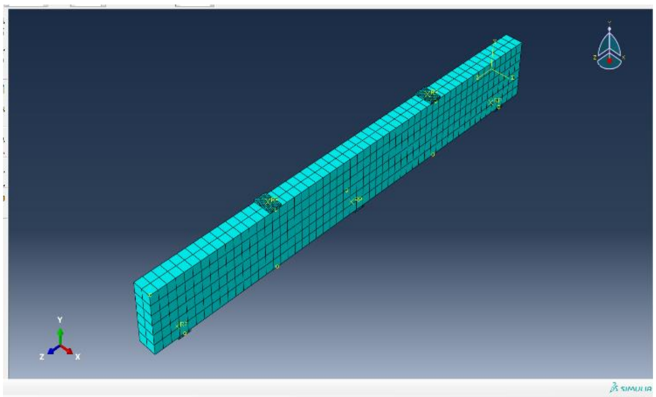

Figure 37 Meshing of Continuous deep beam, FRP reinforcement and bearing plates

The Mesh module is used to generate a finite element mesh on the assembly. Different levels of automation and control are available.

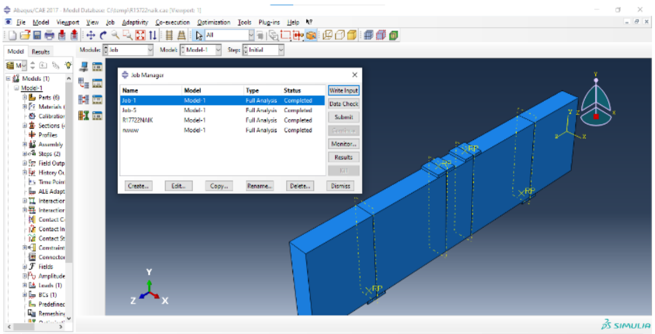

Figure 38 Creating a Job File and Submitting for Analysis.

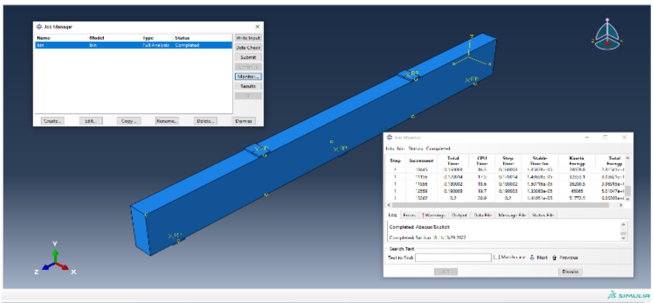

Figure 39 Creating a Job File and Submitting for Analysis.

Creating and Submitting an Analysis Job

A job is created and associated with the model, and then submitted for analysis. The Job module allows for interactive submission and monitoring of the job.

5.5.5 Viewing Results (Visualization)

The Visualization module is used to view the results of the analysis, including:

- Stress
- Strain
- Deformation
- Rotation
- Crack pattern

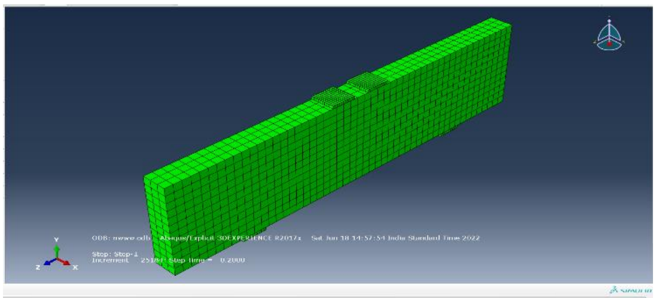

Figure 40 Undeformed Shape Plot of Simply Supported Deep Beam Model

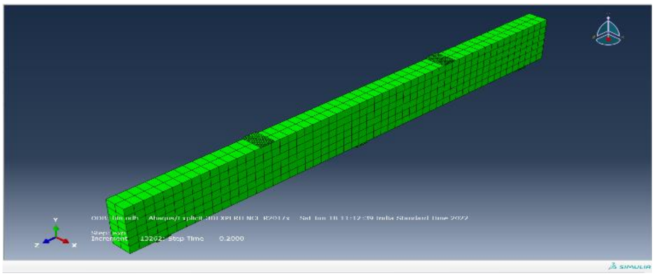

Figure 41 Undeformed Shape Plot of Continuous Deep Beam Model

The module reads the output database (odb) generated during the analysis and displays the results.

6.0 RESULTS

The finite element analysis of deep beams reinforced with Fiber-Reinforced Polymer (FRP) and steel was conducted using ABAQUS/CAE 2017 to investigate their structural behavior.

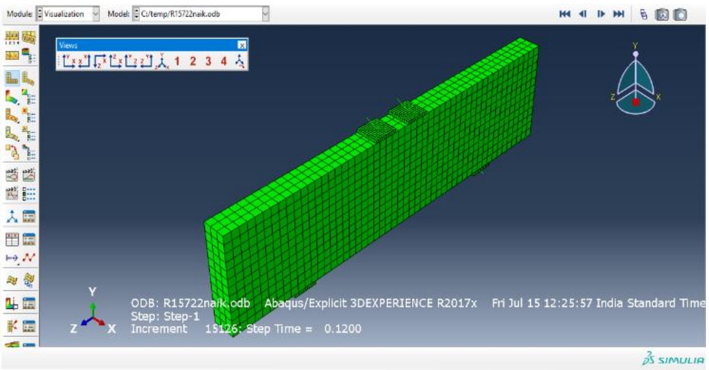

Figure 42 Undeformed Shape Plot of Simply Supported Deep

Beam Model

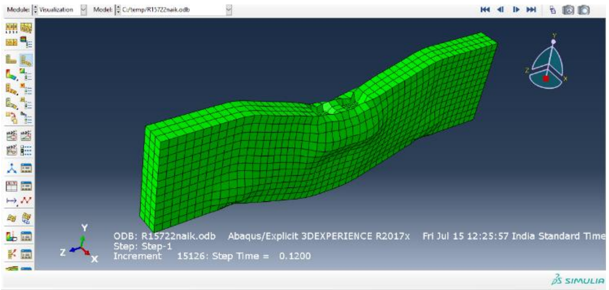

Figure 43 Deformed Shape Plot of Simply Supported Deep Beam Model

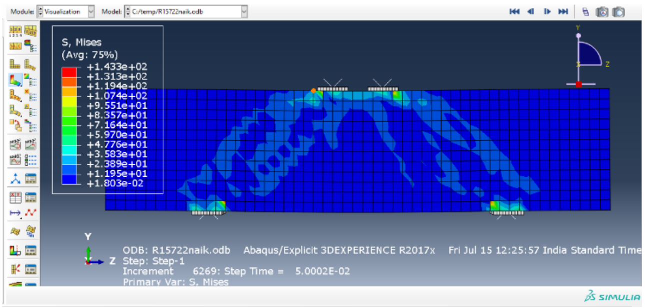

Figure 44 Contour Plot of Mises Stress of Simply Supported Deep Beam Model

6.1 The displacement due to General static and given loading is observed in the following contour diagram.

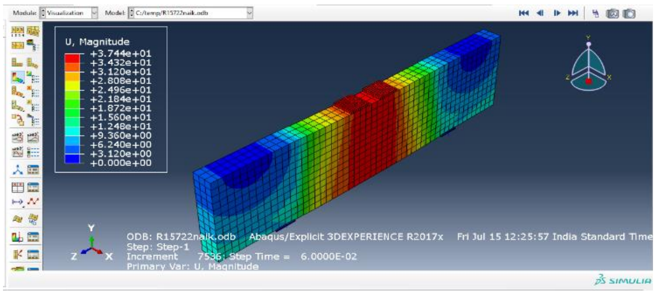

Figure 45 Contour Plot of Deflection of Simply Supported Deep Beam

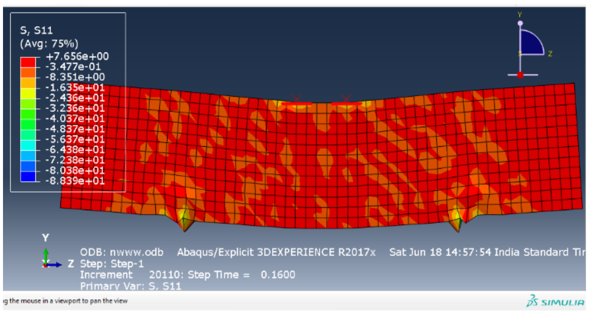

Figure 46 Deformed shape Contour plot of S Mises Stress

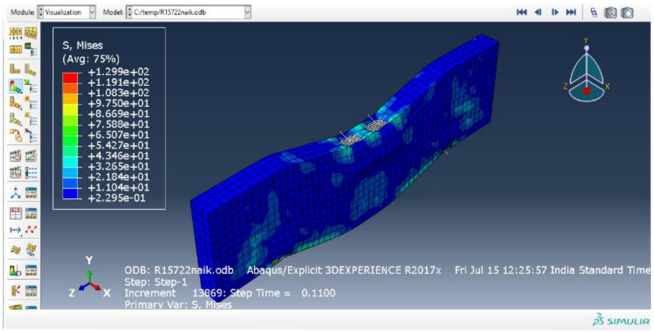

Figure 47 Deformed shape Contour plot of S Mises stress

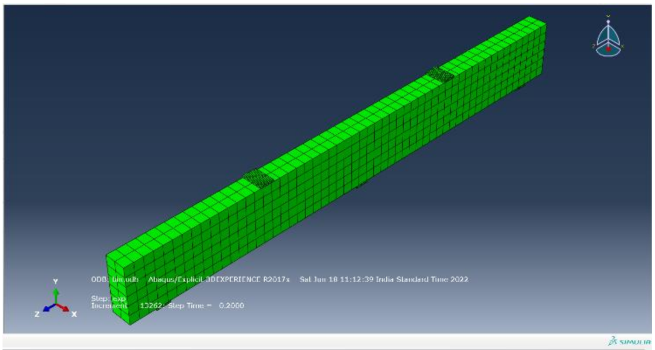

Figure 48 Undeformed shape plot of continuous deep beam model

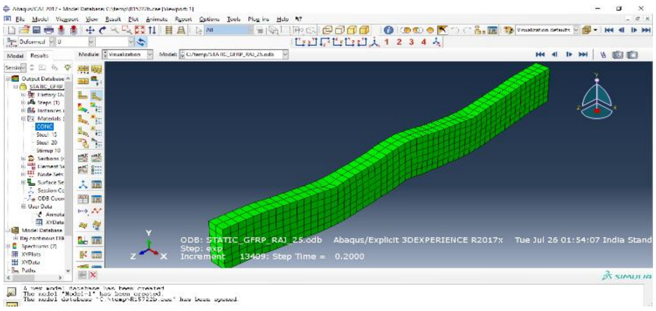

Figure 49 Deformed shape plot of continuous deep beam model

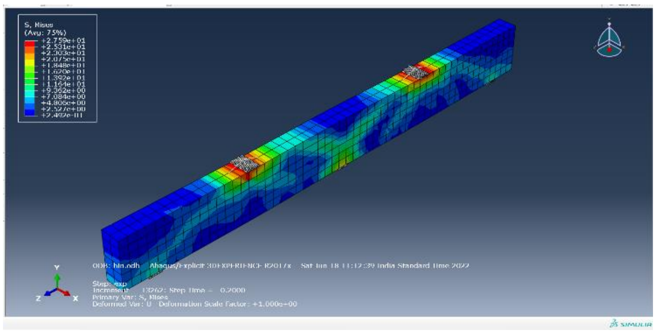

Figure 50 Contour plot of Mises stress of continuous deep beam model

6.2 The displacement due to General static and given loading is observed in the following contour diagram.

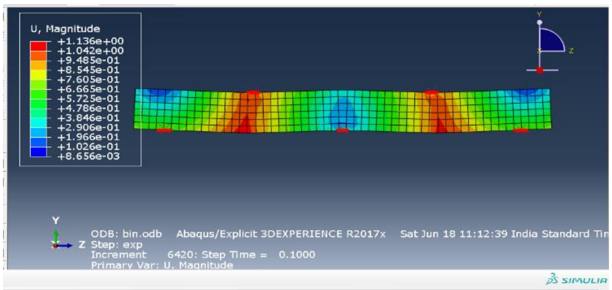

Figure 51 Contour plot of U, magnitude of continuous deep beam mode

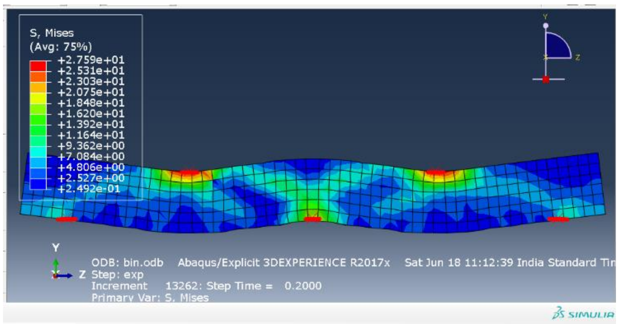

Figure 52 Deformed shape of S,Mises stress diagram

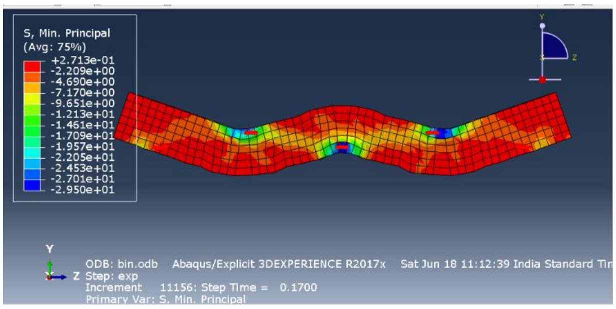

Figure 53 Min.principle stress failure of model

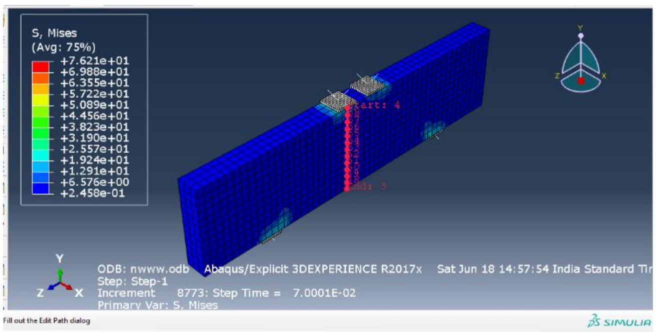

Figure 54 Selected path1 for the field output of the model

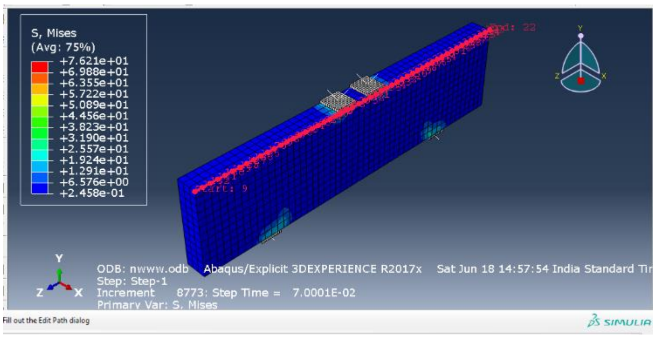

Figure 55 Selected path2 for the field output of the model

6.3 After Completion of analysis part in the post processing step firstly there are contour diagrams in the result visualization section. Thereafter, in the result section we can plot the graphs between various variables such as stress, strain, displacement and force with respect to time and distance or any other variable.

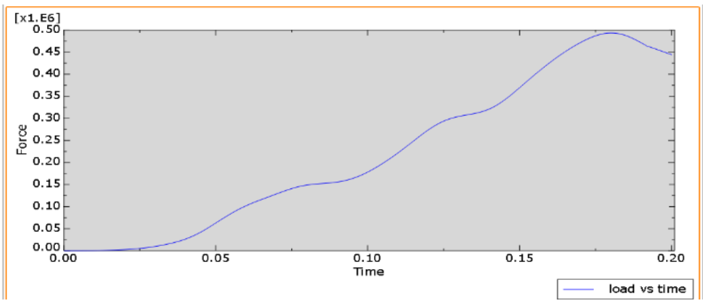

Figure 56 Force (N) vs Time (sec)

For the study of displacement with respect to load at a particular path from the beam we can plot the graph between Load (N) vs Displacement (mm) in the XY plot section. It has been observed that the yielding is occurred at the 759.896 KN load corresponding displacement is 49.5mm and the failure is occurred at the 1567.8 KN load its corresponding displacement is 200 mm.

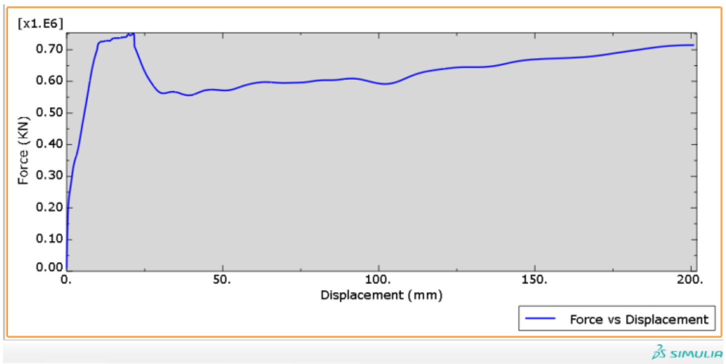

Figure 57 Force (KN) vs Displacement (mm)

For the study of stress vs strain at a particular path in the CFRP reinforced concrete beam from where the stress is maximum, we can plot the graph between Stress (MPa) vs Strain in the XY plot section. It has been observed that the maximum value of stress is 29.341 MPa.

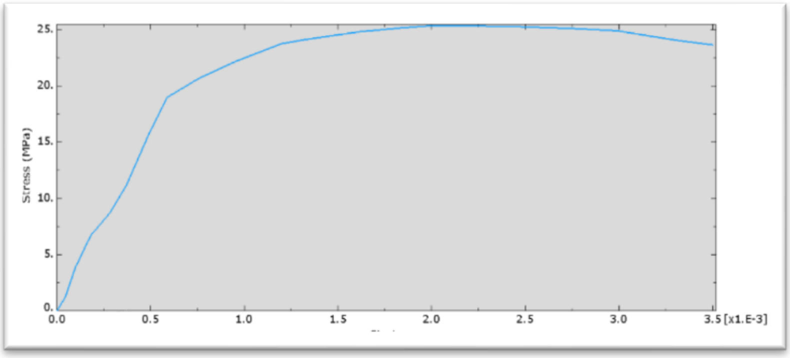

Figure 58 Stress vs Strain

For model-2, Variations of stresses, magnitude, strains and deflections at a selected path1 and path2 of the Continuous deep beam r/f with GFRP has been shown as followings.

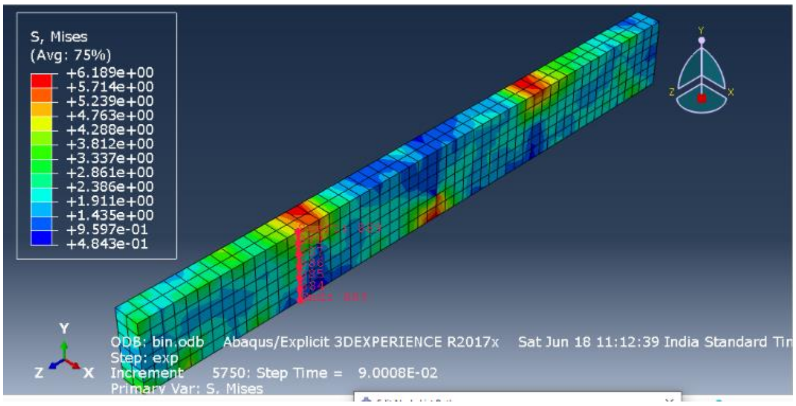

Figure 59 Selected path1 for the field output of the model2

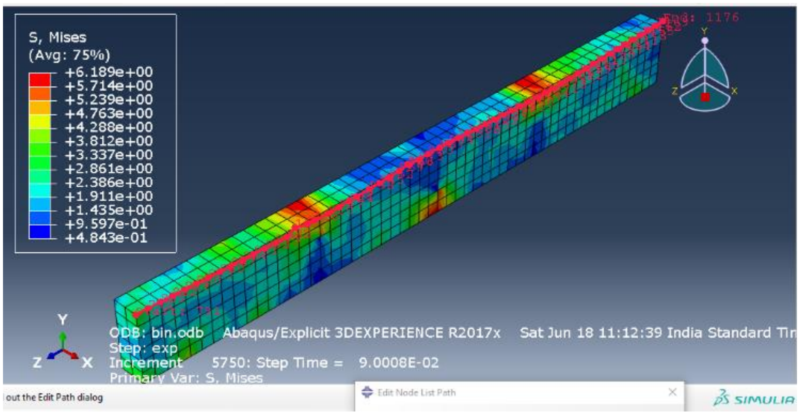

Figure 60 Selected path2 for the field output of the model2

For The result XY plot sections we can plot the graphs between various variables such as stress, strain, displacement, pressure and force with respect to time and distance or any other variable for model-2. The graph between Stress 68.23 (MPa) vs Time (sec) in the XY plot section.

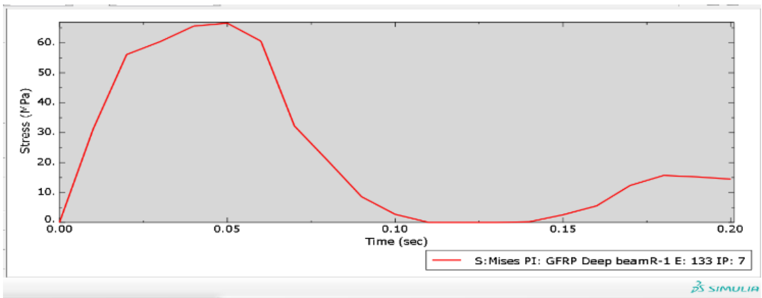

Figure 61 Stress (MPa) vs Time (sec) along path1

For the study of displacement with respect to load at a particular node from composite beam column connection we can plot the graph between Load (N) vs Displacement (mm) in the XY plot section.

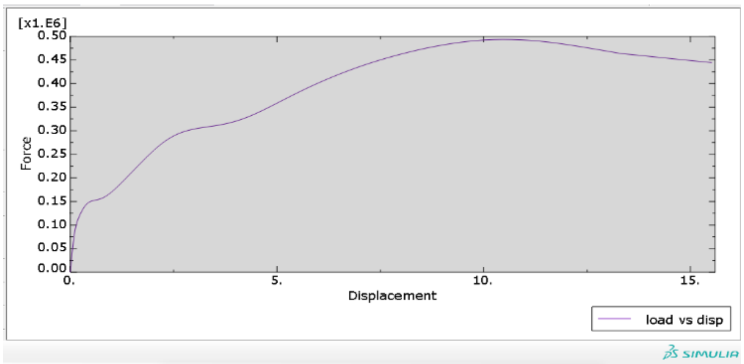

Figure 62 Force (N) vs Displacement (mm)

It has been observed that the yielding is occurred at the 532.543 KN load corresponding displacement is 10.934 mm and the failure is occurred at the 946.894 KN load its corresponding displacement is 68.432 mm.

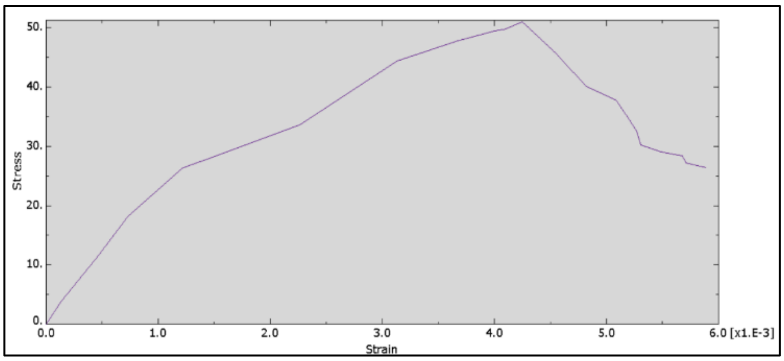

Figure 63 Plot between Stress and Strain.

For the study of stress vs strain at a particular node at the joint location of Composite beam column connection where the stress is maximum, we can plot the graph between Stress (MPa) vs Strain in the XY plot section. It has been observed that the maximum value of stress is 51.0462 MPa.

The findings suggest that FRP reinforced deep beams can be a suitable substitute for conventional steel reinforced deep beams.

The results indicate that FRP reinforced deep beams offer a promising alternative to traditional steel reinforced deep beams.

The study demonstrates the feasibility of using FRP reinforced deep beams as a viable option to replace steel reinforced deep beams.

The outcomes of this research show that FRP reinforced deep beams can be a competitive alternative to traditional steel reinforced deep beams.

7.0 CONCLUSIONS

The finite element analysis of simply supported CFRP-reinforced concrete deep beams and continuous GFRP-reinforced concrete deep beams using ABAQUS/CAE 2017 has led to several significant conclusions:

1. Brittle failure characteristics: The analysis revealed that both beam models exhibited brittle failure, characterized by shear compression and the formation of a major diagonal shear crack, highlighting the need for careful design consideration.

2. Complex failure mechanisms: The study observed multiple failure mechanisms, including shear-compression failure, compression failure of the strut, and diagonal-tension failure, indicating the complexity of deep beam behavior.

3. Arch mechanism formation: The developed strains along the reinforcement and the crack pattern confirmed the formation of the arch mechanism in the beams, indicating efficient load transfer and highlighting the importance of reinforcement detailing.

4. Anchorage effectiveness: The use of headed-end bars prevented end-anchorage failure and slippage of the bottom reinforcement, ensuring secure load transfer and demonstrating the effectiveness of this anchorage system.

5. Shear capacity degradation: The analysis showed that the shear capacity of the beams decreased rapidly with an increase in the shear span-depth ratio (a/d) beyond 2 to 2.5, highlighting the importance of shear span-depth ratio in deep beam design.

6. Reinforcement ratio effects: The reinforcement ratio had no significant impact on the cracking load but substantially affected the ultimate load capacity of the deep beam, demonstrating the importance of reinforcement ratio in deep beam design.

7. Future research directions: This study provides valuable insights into the behavior of deep beams reinforced with FRP, but further research is necessary to investigate the shear behavior of various types of deep beams reinforced with different types of FRP, including the effects of varying material properties, geometric parameters, and loading conditions.

8.0 References

[1] [1] A. S. Farghaly and B. Benmokrane, "Shear Behavior of FRP-Reinforced Concrete Deep Beams without Web Reinforcement," Journal of Composites for Construction, vol. 17, no. 6, Dec. 2013, doi: 10.1061/(asce)cc.1943-5614.0000385.

[2] [2] A. M. Mohamed, K. Mahmoud, and E. F. El-Salakawy, "Behavior of Simply Supported and Continuous Concrete Deep Beams Reinforced with GFRP Bars," 2020, doi: 10.1061/(ASCE).

[3] [3] W. A. Jasim, Y. B. A. Tahnat, and A. M. Halahla, "Behavior of reinforced concrete deep beam with web openings strengthened with (CFRP) sheet," Structures, vol. 26, pp. 785–800, Aug. 2020, doi: 10.1016/j.istruc.2020.05.003.

[4] [4] M. S. Alam, "Assessment of shear capacity of fiber-reinforced polymer deep beams using different methods," ACI Structural Journal, vol. 118, no. 6, pp. 237–250, Nov. 2021, doi: 10.14359/51733079.

[5] [5] K. Mohamed, A. S. Farghaly, and B. Benmokrane, "Effect of Vertical and Horizontal Web Reinforcement on the Strength and Deformation of Concrete Deep Beams Reinforced with GFRP Bars," Journal of Structural Engineering, vol. 143, no. 8, Aug. 2017, doi: 10.1061/(asce)st.1943-541x.0001786.

[6] [6] M. Ibrahim, T. Wakjira, and U. Ebead, "Shear strengthening of reinforced concrete deep beams using near-surface mounted hybrid carbon/glass fibre reinforced polymer strips," Engineering Structures, vol. 210, May 2020, doi: 10.1016/j.engstruct.2020.110412.

[7] [7] T. el Maaddawy and S. Sherif, "FRP composites for shear strengthening of reinforced concrete deep beams with openings," Composite Structures, vol. 89, no. 1, pp. 60–69, Jun. 2009, doi: 10.1016/j.compstruct.2008.06.022.

[8] [8] C. H. Kim and H. S. Jang, "Concrete Shear Strength of Normal and Lightweight Concrete Beams Reinforced with FRP Bars," Journal of Composites for Construction, vol. 18, no. 2, Apr. 2014, doi: 10.1061/(asce)cc.1943-5614.0000440.

[9] [9] A. G. Razaqpur and S. Spadea, "Shear Strength of FRP Reinforced Concrete Members with Stirrups," Journal of Composites for Construction, vol. 19, no. 1, Feb. 2015, doi: 10.1061/(asce)cc.1943-5614.0000483.

[10] [10] J. F. Chen and J. G. Teng, "Shear capacity of FRP-strengthened RC beams: FRP debonding," 2003.

[11] [11] A. F. Ashour, "Flexural and shear capacities of concrete beams reinforced with GFRP bars," Construction and Building Materials, vol. 20, no. 10, pp. 1005–1015, Dec. 2006, doi: 10.1016/j.conbuildmat.2005.06.023.

[12] [12] O. H. Zinkaah and A. Ashour, "Load capacity predictions of continuous concrete deep beams reinforced with GFRP bars," Structures, vol. 19, pp. 449–462, Jun. 2019, doi: 10.1016/j.istruc.2019.02.007.

[13] [13] M. R. Islam, M. A. Mansur, and M. Maalej, "Shear strengthening of RC deep beams using externally bonded FRP systems," Cement and Concrete Composites, vol. 27, no. 3,pp.413–420,Mar.2005,doi: 10.1016/j.cemconcomp.2004.04.002.

[14] [14] M. F. Andermatt and A. S. Lubell, "Behavior of Concrete Deep Beams Reinforced with Internal Fiber-Reinforced Polymer—Experimental Study,"

[15][15] F. Peng, W. Xue, F. Peng, and W. Xue, "Database Evaluation of Shear Strength of Slender Fiber-Reinforced Polymer-Reinforced Concrete Members," ACI Structural Journal, vol. 117, no. 3, pp. 273–281, May 2020, doi: 10.14359/51723504.

[16][16] E. El-Salakawy, B. Benmokrane, and G. Desgagné, "Fibre-reinforced polymer composite bars for the concrete deck slab of Wotton Bridge," Canadian Journal of Civil Engineering, vol. 30, no. 5, pp. 861–870, Oct. 2003, doi: 10.1139/l03-055.

[17][17] Pandey, Ashutosh & Verma, Shashikant & Mehta, Darshan & Azamathulla, Hazi. (2025). A NEW PORTABLE WATER FILTER SYSTEM FOR WASTEWATER. 61. 169-187.

[18][18] A. K. El-Sayed, E. F. El-Salakawy, and B. Benmokrane, "Shear strength of fibre-reinforced polymer reinforced concrete deep beams without web reinforcement," Canadian Journal of Civil Engineering, vol. 39, no. 5, pp. 546–555, May 2012, doi: 10.1139/L2012-034.

[19][19] F. Matta, E. Zappa, F. Mat, A. St Ruct Ural, J. Albert, and R. Garcia, "Size effect on concrete shear strength in beams reinforced with fiber-reinforced polymer bars,"

[20][20] A. H. Zaher, W. M. Montaser, and M. M. Elsonbaty, "STRENGTHENING AND REPAIRING OF RC DEEP BEAMS USING CFRP AND GFRP," International Journal of Civil Engineering and Technology, vol. 11, no. 1, pp. 64–85, 2020.

[21][21] S. Chin, F. Mat Yahaya, D. Shu Ing, and A. Kusbiantoro, "Experimental Study on Shear Strengthening of RC Deep Beams with Large Openings Using CFRP," 2015

[22][22] S. H. Lee, A. Abolmaali, K. J. Shin, and H. du Lee, "ABAQUS modeling for post-tensioned reinforced concrete beams," Journal of Building Engineering, vol. 30, Jul. 2020, doi: 10.1016/j.jobe.2020.101273.

[23][23] Verma, S., D. Mehta, A. Pandey, S.Malani, and R. Pandey. 2024.Flood Hazard: A QGIS Plugin for Assessing Flood Consequences.; Journal of Water Management Modeling 32: C529

[24][24] Aaron Anil Chadee , Shree Ram Malani , Ashutosh Pandey , Shashikant Verma , Anurag Sharma , Darshan Mehta , Tarun Kumar Rajak (2024). Comparison of the Test Results of Conventional Concrete with Sulphur-coated Aggregate Concrete. Civil Engineering and Architecture, 12(5), 3294 - 3305. DOI: 10.13189/cea.2024.120514.

[25][25] https://doi.org/10.36948/ijfmr.2023.v05i04.4783